E-proceedings of the 36th IAHR World Congress
28 June – 3 July, 2015, The Hague, the Netherlands

OPERATIONAL OCEANOGRAPHIC PLATFORM IN THERMAIKOS GULF (GREECE): FORECASTING AND EMERGENCY ALERT SYSTEM FOR PUBLIC USE

YANNIS KRESTENITIS, KATERINA KOMBIADOU, YANNIS S. ANDROULIDAKIS, CHRISTOS MAKRIS, VASSILIS BALTIKAS, CHARALAMBOS SKOULIKARIS, YANNIS KONTOS, GIOLANTA KALANTZI
Laboratory of Maritime Engineering and Maritime Works, Civil Engineering Department, Aristotle University of Thessaloniki, 54124, Thessaloniki, Greece, ynkrest@civil.auth.gr

ABSTRACT

A state-of-the-art forecasting system (WaveForUs: Wave climate and coastal circulation Forecasts for public Use) is implemented, delivering 3-day forecasts of spectral wave characteristics, hydrodynamic circulation and storm surges for the Thermaikos Gulf (North Aegean Sea). The forecasts are disseminated to the public via television broadcasts and internet applications. The WaveForUs platform is fully functional and aspires to provide users with an invaluable tool for their sea-based activities in Greece. The simulations are based on a storm surge hydrodynamic model, a circulation ocean model and a wave model, while necessary atmospheric input data are provided by a well-validated atmospheric model. The main characteristics of the WaveForUs system and the sea-state models that comprise the core of the modelling system are presented and discussed, while results from calibration/validation tests support the accuracy of the forecasts.

Keywords: forecasting system, waves, storm surges, circulation, freshwater fluxes

1. INTRODUCTION

The gulf of Thermaikos (Figure 1), an important environmental and socioeconomic region of the NW Aegean Sea, is an enclosed area with a variety of sea-related activities (transportations, fishing, aquaculture, nautathletic, touristic etc) and, at the same time, is surrounded by a highly populated coastal zone (Thessaloniki, located at its' north-westernmost extremity, is the 2nd largest city of Greece). Three protected wetlands are hosted in its coastal region, while extensive agriculture takes place mainly in the northern part of the adjacent land area. It follows that there is strong interest and need for reliable, high-resolution and site-specific, sea-state forecasts. Aim of the WaveForUs project is to cover these needs, through the development of a high-resolution (1/60ºx1/60º), state-of-the-art, sea-state forecasting system that provides 3-day prognoses of wave, Sea Level Height (SLH), seawater temperature, salinity and current velocities. This paper focuses on the description of the WaveForUs system, and, mainly, on the models used for wave, storm surge and circulation forecast, in terms of parameterizations and effectiveness to reproduce the actual conditions in the field.

Regarding existing operational forecasting systems that overlap spatially with WaveForUs, we note that, currently, 3 such systems exist: (a) the TRITON wave forecasting system[a] (1/90ºx1/90º) that delivers 60-hour wave forecasts in Thermaikos (22.5ºE-23.5ºE and 39.4ºN-40.8ºN), the ALERMO Ocean Forecasting System[b] (1/50ºx1/50º) that delivers 5-day temperature, salinity, current velocity and SLH forecasts in the Aegean-Levantine area (20ºE-36.4ºE and 30.7ºN-41.2ºN) and (c) the POSEIDON system[c] (1/30ºx1/30º) that delivers 5-day forecasts of wave, temperature, salinity, current velocity and SLH fields in the Aegean Sea (19.5ºE-30ºE and 30.4ºN-41ºN). TRITON, on one hand, provides higher spatial resolution, but on the other hand, is limited only to wave forecasts and there is no available validation of the forecast product. ALERMO provides similar, but lower-resolution, circulation forecasts and, at the same time, the available results for the 3-dimensional parameters are provided for the depths of 5, 30, 120 and 360m; apart from the 5m layer, these depths are well over the depth-range of the Thermaikos gulf, and, therefore, these prognoses are of no interest to a local user. POSEIDON is a well-documented and highly-reliable system (Korres et al., 2008) that produces results for all of the WaveForUs forecast parameters. However, its resolution is significantly lower (1:4), while, for the depth-varying parameters (physical properties and currents), POSEIDON offers results only for the surface layer. It follows that WaveForUs has advantages over all of the existing operational systems in the area and the need for its development is indeed substantiated.

Regarding the structure of the present paper, in the methodology section (Section 2), we present the general characteristics of the system, regarding models used, application domains, inter-model transfer of input and coupling data, followed by a detailed presentation of the characteristics of each of the 3 sea-state models. In Section 3, we present calibration and validation results from available measured data for each model, as well as indicative results from

[a] http://www.oc.phys.uoa.gr/dok1.htm
[b] http://www.oc.phys.uoa.gr/oceanf.html
[c] http://poseidon.hcmr.gr/

the 3-day operational forecasts. Sections 4 and 5 are dedicated to the discussion of the effectiveness of the system and future work and to the concluding remarks of the work, respectively.

2. METHODOLOGY

The two main components of the WaveForUs system, shown schematically in Figure 1, are the modelling and forecast dissemination platforms. In the present paper we focus mainly on the former, while the latter is described in brief. The WaveForUs modelling platform consists of the following four mathematical models (Figure 1), one atmospheric and three sea-state models. The meteorological model used is the Weather Research and Forecasting model with the Advanced Research dynamic solver (**WRF-ARW**; Pytharoulis et al., 2014; Wang et al., 2010). For the simulation of wave climate the WaveWatch-III, version 3.14 (**WW-III**; Tolman, 2009) model is applied, whereas storm surges in the area are simulated through the High Resolution Storm Surge (**HRSS**; Krestenitis et al., 2011) model and coastal circulation is modeled using the Princeton Ocean Model, version 2008 (**POM**; Blumberg and Mellor, 1987).

The models are applied in three domains of gradually increasing discretisation (Figure 1):

- Mediterranean Sea (Domain 1) with a step of 0.15°x0.15° (~15km),
- Aegean Sea (Domain 2) with a step of 0.05°x0.05° (~5km) and
- Thermaikos Gulf (Domain 3) with a step of 0.016°x0.016° (~1.7km).

Boundary conditions are transferred from coarser to the finer domains, while atmospheric input parameters for the sea-state models are obtained by the application of WRF-ARW in each domain (Figure 1). It is noted that WW-III is not applied in Domain 1, since preliminary applications of the model showed that an inclusion of the Mediterranean Sea has practically no effect to the wave forecasts in the Thermaikos domain. POM is only applied in Domain 3 and receives boundary conditions (sea level, temperature, salinity and horizontal velocity fields) from the MyOcean system[d]. One-way coupling between the sea-state models is currently underway and includes the provision of SLH data from HRSS to WW-III, for the correction of seawater depths at all grid cells, and the addition of Stokes drift velocities calculated by WW-III to POM, for the improvement of current velocity approximation.

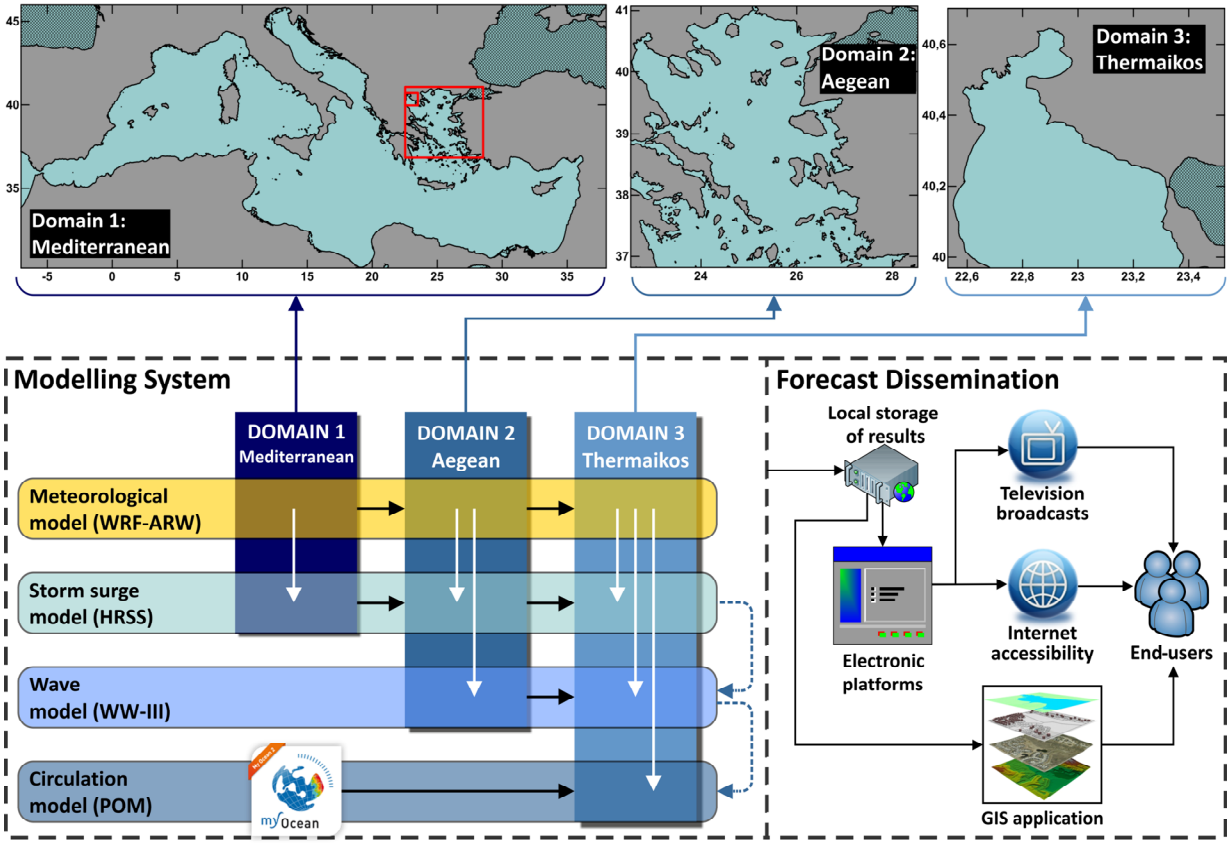

Figure 1. Schematic representation of the WaveForUs forecasting system: The lower panel (left part) shows the numerical models used in each application domain and the transfer of data within the system (black arrows denote transfer of initial and boundary conditions, white ones introduction of input data and blue-dashed arrows denote inter-model coupling) and the dissemination of forecast products (right part), while the upper panel shows the location of the three application domains (hatched areas aren't included in the calculations).

[d] http://www.myocean.eu

The system is currently operational and delivers 3-day prognoses of wave fields (significant wave height and direction), SLHs and circulation parameters (currents, temperature and salinity fields) that are updated daily at 08:30 UTC. Dissemination of forecast products (Figure 1) is performed through the following 3 routes: **a)** the web Geographical Information System (GIS) platform of the project[e], **b)** the television broadcasts of DION-TV[f] and **c)** the WaveForUs webpage[g]. Following, we discuss the main characteristics of the sea-state models. It is noted an alert system for strong surges that reach coastal waters of Thermaikos Gulf is also included in the system. More specifically, using the forecasts of WW-III, the wave setup and surf beat are calculated for all coastal cells of Domain 3; these values are added to the simulated SLHs, derived by the HRSS model that takes into account astronomical and meteorological tides, as analysed further below, in order to estimate the total setup at each coastal cell. In cases of high total setup values in low elevation coastal areas, coastal inundation risk bulletins are issued by DION-TV, in addition to the daily scheduled broadcasts.

2.1 Wave model

WW-III is a well known and widely used third generation spectral model for the simulation and prognosis of wind-generated wave fields, developed at the Marine Modeling and Analysis Branch (MMAB) of the National Center for Environmental Prediction (NCEP)[h]. The governing equation of WW-III is the balance equation of the wave action density spectrum $N(k,\theta)=F(k,\theta)/\sigma$, where $F(k,\theta)$ is the wave variance density spectrum and σ the intrinsic frequency. In cases with ambient currents present, wave action is a conserved quantity (Whitham 1965, Bretherthon and Garret 1968), and that is the reason for $N(k,\theta;\mathbf{x},t)$ being the spectrum of choice within the model.

WW-III can be run on either Cartesian or spherical grids. In our case the selected geographical grid formulation was that of a spherical grid. The wave action balance equation for spherical coordinates can take the following form:

$$\frac{\partial N}{\partial t}+\frac{1}{\cos\varphi}\frac{\partial}{\partial\varphi}\left(\dot{\phi}\cdot N\cdot\cos\theta\right)+\frac{\partial}{\partial\lambda}\left(\dot{\lambda}\cdot N\right)+\frac{\partial}{\partial k}\left(\dot{k}\cdot N\right)+\frac{\partial}{\partial\theta}\left(\dot{\theta}_g\cdot N\right)=\frac{S}{\sigma}$$

$$\text{and}\left\{\begin{array}{ll}\dot{k}=-\dfrac{\partial\sigma}{\partial d}\dfrac{\partial d}{\partial\sigma}-\mathbf{k}\dfrac{\partial \mathbf{U}}{\partial s} & \dot{\phi}=\dfrac{c_g\cdot\cos\theta+U_\varphi}{R}\\ \dot{\theta}=-\dfrac{1}{k}\left[\dfrac{\partial\sigma}{\partial d}\dfrac{\partial d}{\partial m}-\mathbf{k}\dfrac{\partial U}{\partial m}\right] & \dot{\lambda}=\dfrac{c_g\cdot\cos\theta+U_\lambda}{R\cdot\cos\varphi}\\ & \dot{\theta}_g=\dot{\theta}-\dfrac{c_g\cdot\tan\varphi\cdot\cos\theta}{R}\end{array}\right\} \qquad [1]$$

where s is a coordinate in the direction θ, m is a coordinate perpendicular to s, λ and φ are the geographical longitude and latitude respectively, R is the earth's radius and U_φ and U_λ are the current components, if currents are present. The governing equation accounts for refraction and straining of the wave field due to temporal and spatial variations of the mean water depth and of the mean current. The physical processes of wave growth and decay due to the actions of wind, non-linear resonant interactions, dissipation (`whitecapping'), bottom friction, surf-breaking (i.e., depth-induced breaking) and scattering due to wave-bottom interactions, are accounted for by the means of various source terms which are included in S, that represents the net effect of sources and sinks for the spectrum F.

The wave model is set-up using the bathymetries of the two smaller domains of our simulations, Domain 2 for the North Aegean sea and Domain 3 for the Thermaikos Gulf. The spatial discretization of the grids, used by the model, is the same as for the rest of the numerical models in each domain, as previously mentioned mentioned. The model's wind input are all the wind fields for the two domains, with an hourly time step, produced by the WRF meteorological model. These wind fields are then interpolated by the models' algorithm, using the options of linear interpolation and approximately linear interpolation in time and space respectively.

Calculations start from initially calm conditions (H_s =0), using the available spectral seeding option and are then carried out, using the ULTIMATE QUICKEST propagation scheme with the Tolman averaging technique (Tolman 2002a) and the WAM4 and variants source term package of input and dissipation with the stability correction for this package (Abdalla and Bildot 2002) enabled as an option in the model. The Battjes-Janssen depth-induced wave breaking is employed and the Jonswap formulation is used for the inclusion of bottom friction. As far as the non-linear resonant and near-resonant wave-wave interactions are concerned, triad wave-wave interactions are not included in the calculations, whereas four wave-wave interactions are taken into account by the means of the Discrete Interaction Approximation (DIA). Results for the Thermaikos Gulf are obtained after nested runs of the WW-III model, using its two-way nesting feature introduced in version 3.14 (Tolman, 2006, 2007, 2008). Since the calculations start from initially calm conditions, the first 15 of the models' hourly output datasets are discarded, to ensure that the model output forecasts refer to fully developed wave fields.

2.2 Storm surge

[e] http://ecoplan.static.otenet.gr:8079/WForUsApp/AppStart.html
[f] http://www.diontv.gr/index.php/eidiseis-apo-tin-dion-tileorasi-2/wave-4-us
[g] http://wave4us.web.auth.gr/index_eng.html
[h] http://polar.ncep.noaa.gov/waves/

2.2.1 Model description

The storm surge simulations are based on a 2-dimensional HRSS (De Vries et al., 1995; Krestenitis et al. 2010), implemented in the 3 domains (Figure 1). The model solves the shallow water equations and computes the sea surface elevation in every cell of the domain. The model solves the shallow water equations and computes the sea surface elevation in every cell of the domain. The Smagorisky coefffficient (CCC) is set equal to 0.10 (Rogallo and Moin, 1984) in the calculation of turbulent eddy viscocity. The main equations of the mathematical model are the momentum (Eqs. [2] and [3]) and continuity (Eq. [4]) equations:

$$\frac{\partial u}{\partial t}+u\frac{\partial u}{\partial x}+v\frac{\partial u}{\partial y}-fu+g\frac{\partial z}{\partial x}=-\frac{1}{\rho_o}\frac{\partial P}{\partial x}+\frac{1}{\rho_o}\frac{\tau_\chi}{(h+z)}-k\frac{u\sqrt{u^2+v^2}}{\rho_o(h+z)}-\frac{g}{\rho_o}\frac{0.9\partial z-0.7\partial z_o}{\partial x} \quad [2]$$

$$\frac{\partial v}{\partial t}+u\frac{\partial v}{\partial x}+v\frac{\partial v}{\partial y}+fu+g\frac{\partial z}{\partial y}=-\frac{1}{\rho_o}\frac{\partial P}{\partial y}+\frac{1}{\rho_o}\frac{\tau_y}{(h+z)}-k\frac{u\sqrt{u^2+v^2}}{\rho_o(h+z)}-\frac{g}{\rho_o}\frac{0.9\partial z-0.7\partial z_o}{\partial y} \quad [3]$$

$$\frac{\partial z}{\partial t}+\frac{\partial (h+z)u}{\partial x}+\frac{\partial (h+z)v}{\partial y}=0 \quad [4]$$

where t is the time, x,y are the spatial coordinates, z is the water level elevation above the mean sea level, u-v are the x-y components of the depth-mean current, h is the undisturbed water depth, g is the acceleration of gravity, f is the Coriolis parameter, k is the bottom friction coefficient, τ_X and τ_Y are the x and y components of the wind stress, ρ_o is the density of the water, P is the atmospheric pressure at sea level and z_o is the astronomical tide elevation. The calculation of the wind stress fields is based on the transformation wind velocity data at 10m, to the zonal/meridional components of the wind stress exerting on the sea surface, according to the formula of Eq. [5].

$$\tau=\rho_A C_D \mid W \mid W \quad [5]$$

where ρ_A is the air density, W is the wind velocity and C_D is the surface friction coefficient. Wave radiation stresses used in momentum equations were calculated from the wave height and direction for each grid cell and time step. Experiments with various values of the surface friction coefficient were executed, including the calculation of C_D, according to Eq. [6] (Smith and Banke, 1975).

$$C_D=(0.63+0.066W)/10^3 \quad [6]$$

The simulations of Domain 1 provide the boundary conditions to Domain 2 and successively to Domain 3 (Thermaikos Gulf). The nesting approach is based on the open boundary condition, where the elevation of the sea surface is given by the outer model. The condition of the sea surface elevation in the open boundary is based on the combination of two computation approaches of the vertical velocity to the boundary. In the first approach, the vertical velocity V is based on the Sommerfeld radiation condition. In the second approach, the velocity V is calculated by the Neumann condition.

2.2.2 Tidal parameterization

The contribution of the astronomical tide is calculated at every cell of the grid based on the Schwiderski (1980) parameterization and is included in the momentum equations. The tide forecast is based on the solution of harmonic equation at all grid longitudes and latitudes. The semi-diurnal signal of the tide is measured in meters and is calculated by Eq. [7]. Moreover, the diurnal signal is calculated by Eq. [8].

$$n=k_o \sin^2(\varphi)\cos(\sigma t+x+2\lambda) \quad [7]$$

$$n=k_o \sin(2\varphi)\cos(\sigma t+x+\lambda) \quad [8]$$

where the width of the tide balance is k_o=0.242334 m, the frequency σ=1.40519·10-4 s^{-1} and the astronomical argument for M_2 tidal mode at 00:00 GMT is derived by $x=2\cdot h_o-2\cdot s_o$. Similarly, the S_2, N_2, K_2, K_1, O_1, P_1, Q_1 tidal modes are given by Schwiderski (1980). φ and λ are the geographic longitude and latitude of each cell. The mean distances of sun h_o and moon s_o are given by:

$$h_o=279.69668+36000.768930485T_d+3.03*10^{-4}{T_d}^2 \quad [9]$$

$$s_o=270.434358+481267.88314137T_d-0.001133{T_d}^2+1.9\cdot 10^{-6}{T_d}^3 \quad [10]$$

$$T_d=(27392.500528+1.0000000356D)/36525 \quad [11]$$

$$D=day+365\cdot(yr-1975)+\text{int}[(yr-1973)/4] \quad [12]$$

where day is the number of year day (day=1 on 1st January) and yr is the study year from 1975.

2.3 Ocean circulation modelling

2.3.1 Princeton Ocean Model

The widely applied and validated Princeton Ocean Model (POM; Blumberg and Mellor, 1987) is used for forecasting coastal circulation. POM is a three-dimensional, free-surface, terrain-following model, suitable for coastal and estuarine areas. In WaveForUs, POM is applied only in Domain 3 (Thermaikos gulf) using 16 vertical sigma layers, while boundary conditions regarding SLH, velocity, temperature and salinity fields are obtained by the MyOcean system. POM also receives all the necessary input atmospheric parameters, including wind velocities, atmospheric pressure, temperature, humidity and precipitation fields, as well as thermal and radiation fluxes, from the WRF-ARW forecasts.

Regarding thermal heat exchanges at the free surface, the related heat balance at the boundary, assuming an upward positive sign (i.e. the water column is warming when the $Q_{flux,surf}$ is negative), is written:

$$Q_{flux,surf} = -Q_{SWR} + Q_{LWR} + Q_{SH} + Q_{LH} \quad [13]$$

where Q_{SWR} and Q_{LWR} are the net upward Longwave and Shortwave Radiation fluxes and Q_{SH} and Q_{LH} are the sensible and latent heat fluxes, respectively. Radiation fluxes are directly obtained by WRF-ARW, while the heat fluxes (Q_{SH} and Q_{LH}) are expressed using the following formulas (Weare et al., 1981; Rosati and Miyakoda, 1988):

$$Q_{SH} = \rho_\alpha c_p c_H |W|(T_s - T_\alpha) \quad [14]$$

$$Q_{LH} = \rho_\alpha \cdot L \cdot c_E |W|\left(e_{sat}(T_s) - r \cdot e_{sat}(T_\alpha)\right) 0.622 / p_a \quad [15]$$

$$L = 2.501 \cdot 10^6 - 2.3 \cdot 10^3 T_s \quad [16]$$

where ρ_α is the air density, c_E and c_H are turbulent exchange coefficients (c_E=c_H=1.1·10^{-3}), c_p is the specific heat capacity (c_H=1005 J/kg/K), $e_{sat}(T_s)$ and $e_{sat}(T_\alpha)$ are the saturation water vapor pressure for the sea and the atmospheric temperature (T_s and T_α), L is the latent heat of vaporization (Eq. 16; Gill, 1982), r is the relative humidity (provided by WRF-ARW) and p_α is the atmospheric pressure. The saturation water vapor pressure is calculated after Lowe (1977).

Another important factor for the circulation and seawater properties in the area if the freshwater flow in Thermaikos from the 3 main rivers, namely Axios, Loudias and Aliakmon, that form an elaborate deltaic system in the NW coasts of the gulf (Figure 2a). The lack of measurements regarding their freshwater fluxes, on one hand, and the presence of consecutive hydropower-water supply dams along the two main rivers (Axios and Aliakmon) and the irregularity in the discharges of the other (Loudias mainly acts as a drainage canal), made it necessary to develop a methodology for the estimation of the freshwater supplies that reach the sea; this methodology is analyzed in the following part of the paper.

2.3.2 River discharge forecasts

The significant differences between the characteristics of the 3 main rivers discharging into the Thermaikos Gulf, one holistic and horizontal simulation approach could not be implemented; more specifically, Axios is a transboundary river, with the upstream head waters, located in FYROM, to control the water volumes that finally reach the sea, Loudias currently acts as the main drainage channel for the surrounding agricultural areas and Aliakmon is fragmented and controlled by seven large dams. Thus, three independent but interconnected methodologies were proposed for the assessment of the outlets of the rivers.

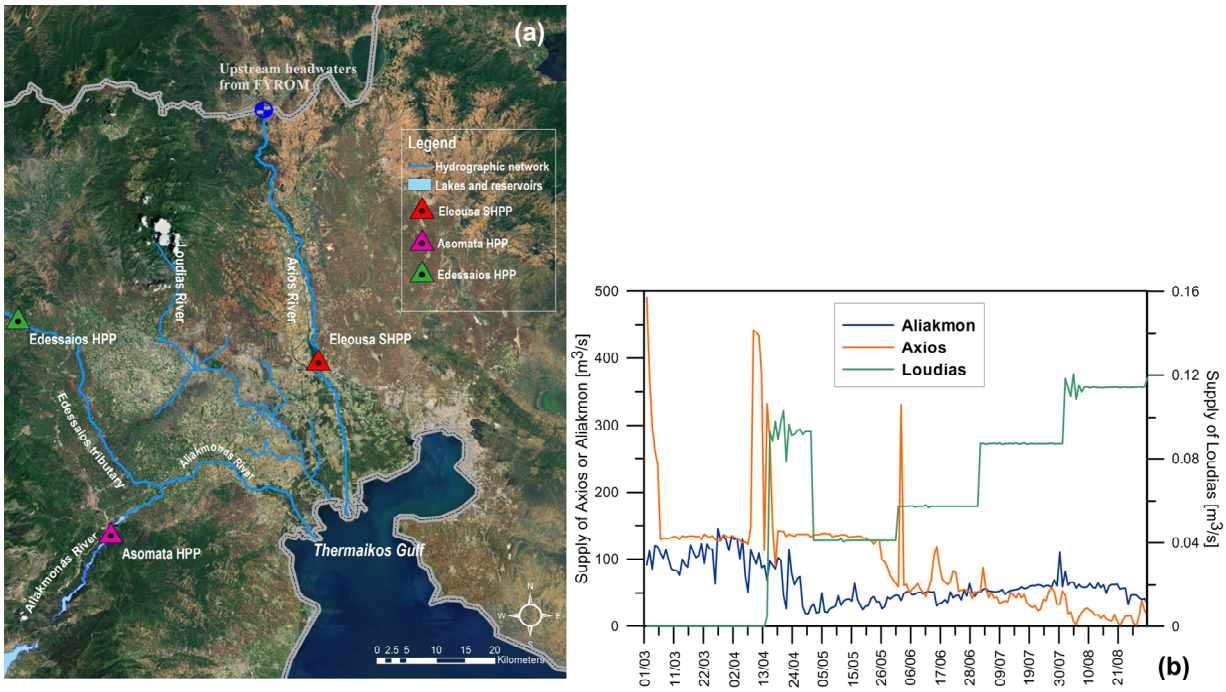

Figure 2. Map of the location main dams along the main route and tributaries of the 3 rivers of Thermaikos (a) and time-series of calculated freshwater supplies (b); due to different magnitudes, the supplies of Loudias refer to the left-hand axis in b.

Regarding Aliakmon, the estimation of freshwater volumes, released downstream from the hydro power plants, is based on two European Union Directives, the River Basin Management Plans (RBMPs) of the Water Framework Directive and the European Network of Transmission System Operators for Electricity of Electricity Market Directive. More specifically, historic power production data from the two downstream hydroelectric power plants (HPPs), namely Assomata and Edessaios dams (Fig. 2a), were retrieved through custom-developed software from the National Transmission System Operator (NTSO) web platform for a ten year period (2004-2013). Thereafter, power was converted to discharges, taking into account the hydraulic head and the turbine efficiency for each dam. The same procedure is followed for retrieving the short-term power production forecasts, published by NTSO. On the other hand, RBMPs were exploited for indentifying water usage, water demands and water sources for covering the demands. Consequently, the total water supply (provided by the NTSO) and demands (coming from the RBMP of Aliakmon) were used for evaluating the water balance and the water volumes that reach the sea.

In the case of the Axios, the lack of data for the upstream part of the basin was an impeding factor for the integrated simulation of the basin, thus emphasis was given to the region downstream from the irrigation dam of Eleousa . Eleousa dam (Fig. 2a) is located 18 km upstream from the estuaries and regulates the water volumes diverted for irrigation purposes and also released to the main river course. The dam has 8 Tainter type gates which control the dam's outlets to the river, with the discharge for this type of gates (Q_{Axios}, in m^3/sec) to be given by the following equation (USACE, 2000):

$$Q_{Axios} = C_{Diss} G_o B \sqrt{2gH_W} \qquad [17]$$

where C_{Diss} is the discharge coefficient, G_o the vertical opening of the gate [m], B the width of the gate [m], g the acceleration due to gravity, H_W the water height upstream from the gate [m]. C_{Diss} and B values are known from the literature, therefore the developed methodology focused on estimating G_o and H_W, in order to estimate the released discharges to the sea. Initially, based on a limited number of records (2010-2011) regarding the opening of the gates and the water height upstream from the gates, a relationship model was built for estimating the discharges in different openings of the gates and water heights. At a second step, water level data at the borders of FYROM and Greece, obtained through a telemetric level sensor, were used for the construction of a relationship table that indicates the height of the water upstream of the gates at different water levels at the border. Thus, continuous water levels at the border are correlated with the relationship tables for assessing the water releases to the main river course. The average time lag of the flow between borders and dam was estimated up to 8 hours.

Finally, for Loudias (Fig. 2a), which, as aforementioned is an ephemeral river (discharges appear only during the irrigation period), the discharges where estimated at 1/3 of the irrigation discharges, after Latinopoulos and Krestenitis (2001). Thus, based on the RBMPs of Aliakmonas and Axios, the areas which drain into the Loudias River were identified and the corresponding irrigation supplies from the two rivers are used for the computation of the drainage discharges.

The time-series of freshwater supplies for the period of 01/03 to 31/08/2013, as derived by the proposed methodology and used in the present analysis, are given in Figure 1b.

3. RESULTS

3.1 Model Evaluation

3.1.1 Wave model validation

Due to the lack of station wave measurements in Thermaikos Gulf and the sparsity of such measurements in the North Aegean Sea, the model's output significant wave height (H_s [m]) was validated by comparison with satellite data. The latter were obtained from the available satellite tracks of Jason-2 / Phase A along the Aegean Sea, for the time period from 3/1/2013 until 2/28/2014. Zero values and outliers from the satellite data were discarded as false. It should be noted that, the measurements of H_s along the satellites' trajectories are separated by a time difference of about 60 seconds. In order to perform collocation over time between the satellite data and the model's output, the satellite data that were eventually used, were those which were obtained within a 20-minute interval from the moments in time of the model's output. The latter has a six-hourly time step. Collocation over space was achieved by requesting WW-III to perform internal spatial interpolation of the results, so that the coordinates of the output coincide with those of the satellite measurement points. The final dataset contains 3724 points. The same procedure was executed in order to compare the model's input wind speed (U_{10} [m/s]) and the wind speed calculated from the satellite measurements.

As shown in Figure 3a, the measured and modeled values of significant wave seem to be in fair agreement (y=0.95x), bearing in mind that satellite algorithm data may contain significant errors. It should be noted, that the largest dispersion of H_s values is restrained within the range of up to 2 m of significant wave height, thus weighing in favor of the model's calculations. Figure 3b shows the correlation f satellite-measured (Jason 2) and input of WW-III wind speed (U_{10} [m/s]) for the 2013 simulation in Domain 2. The fact that there seem to be some differences between the satellite measured data -which are a near real time approximation of the actual wind fields over Domain 2- and the input wave fields of WW-III, gives reason to the differences between the satellite measured and modeled values of H_s, provided that satellite data are in close proximity with the wave heights of the actual wave fields.

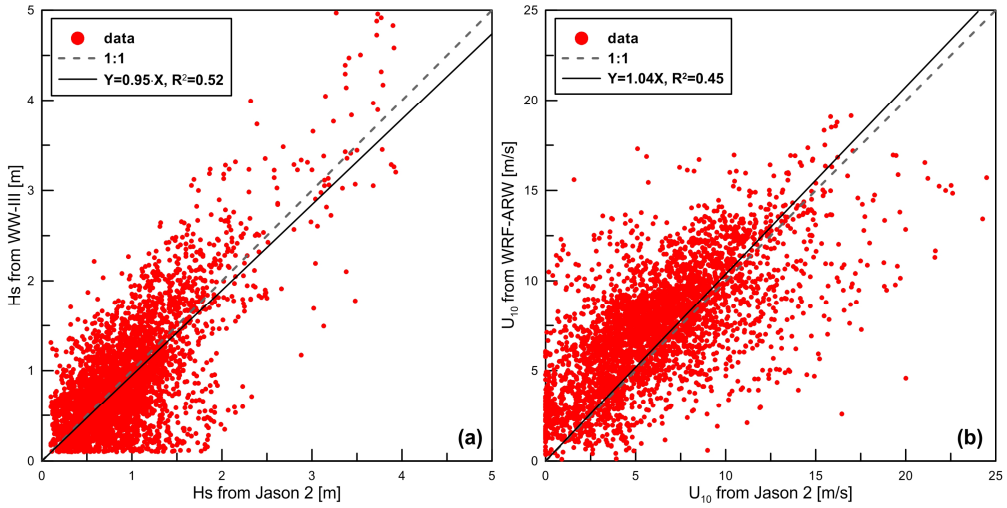

Figure 3. Correlation of satellite-measured (Jason 2) and simulated (WW-III) significant wave height (Hs, [m]) in (a) and satellite measured (Jason 2) and simulated (WRF-ARW) wind velocity at 10m above sea level (U10, [m/s]) in (b) for the 2013 simulation in Domain 2.

3.1.2 Storm surge hindcasting

We simulated the sea level evolution for the year 2012, when available measurements from the tide gauge stations of Thessaloniki (Thermaikos Gulf; Hellenic Navy Hydrographic Service[i]) and Ancona (North Adriatic Sea; Istituto Superiore Per La Protezione e la Ricerca Ambientale[j]) were used in order to calibrate and evaluate the storm surge model for Domain 1 (Mediterranean Sea). The final selected set-up of the model was also applied to the implementation of the model in Domain 2 (Aegean Sea) and Domain 3 (Thermaikos Gulf). The calibrated simulation platform is finally used in operational mode (please see Section 3.2) in order to daily predict the sea level alteration during the future 3-day period. Several experiments were conducted in order to investigate different parameterizations of the model, related to the maximum computation depth, tidal signal, the atmosphere-ocean interaction etc. The 12 experiments with their respective characteristics are briefly presented in Table 1. We checked the performance of the model with realistic or

[i] http://www.hnhs.gr/portal/page/portal/HNHS
[j] http://www.isprambiente.gov.it/

specific maximum depth (e.g. experiments 7 and 8). The open boundary in Gibraltar was also under investigation by applying the harmonic equation with tidal parameters derived from the Huelva gauge station (e.g. Experiment 2). The significant contribution of the wind forcing on the variability of the sea surface elevation was also examined by applying different surface drag coefficients C_D (constant or based on the wind speed, e.g. Smith and Banke (1975)). Moreover, the tide parameterization by Schwiderski (1980), presented in Section 2.2.2, was tested in order to include the contribution of astronomical tidal signal in the simulation of sea elevation in all cells and in every computational time step. Experiment 11 examines the value of Smagorisky coefffcient (CCC) in the calculation of turbulent eddy viscosity.

Table 1. Main characteristics of HRSS experiments for the 2012 period simulations.

EXP #	ATMOSHPERIC FORCING	TIDE SCHWIDERSKI (1980)	GIBRALTAR BOUNDARY	OTHER PARAMETERISATIONS	MAXIMUM DEPTH H
1	YES	NO	NO	C_D (Smith and Banke, 1975)	Realistic
2	YES	NO	YES	C_D (Smith and Banke, 1975)	Realistic
3	YES	YES	NO	C_D (Smith and Banke, 1975)	Realistic
4	YES	YES	YES	C_D (Smith and Banke, 1975)	Realistic
5	YES	NO	NO	$C_D = 10^{-5}$	Realistic
6	YES	NO	NO	$C_D = 10^{-6}$	Realistic
7	YES	NO	NO	C_D (Smith and Banke, 1975)	100
8	YES	NO	NO	$C_D = 10^{-5}$	100
9	YES	YES	YES	$C_D = 10^{-5}$	Realistic
10	YES	YES	YES	$C_D = 10^{-6}$	Realistic
11	YES	NO	NO	C_D (Smith and Banke, 1975) Eddy Viscosity (CCC=0.24)	Realistic
12	YES	YES	YES	$C_D = 10^{-5}$	Realistic

In order to assess the model performance, the Willmott Skill (WS) score was calculated for all experiments (Table 2) after the equation (Liu et al., 2009):

$$WS = 1 - \frac{\sum \left| X_m - X_o \right|^2}{\sum \left(\left| X_m - \overline{X_o} \right| + \left| X_o - \overline{X_o} \right| \right)^2} \quad [18]$$

Where X is the parameter used (in this case SLH), the subscripts o and m indicate observed and modelled value, respectively, and the overbars denote average value. The highest value (WS=1) means perfect agreement between model and observation, while the lowest value (WS=0) indicates complete disagreement.

The Willmott Skill (WS) score (Eq. [18]) as derived from simulated and measured SLHs was computed for Experiment 9, where the surface drag coefficient is equal to 10^{-5} and realistic bathymetry is used. The tide contribution is based on Schwiderski (1980) parameterization and the tidal harmonic equation is applied for Gibraltar open boundary. The total high score is 0.67, while the lowest is derived from Experiment 1. Comparisons between the experiments are used to calibrate all the tested attributes of the model. For example, the use of high fixed drag coefficient equal to 10^{-5} (Experiment 5) revealed higher scores than the respective experiment with low coefficient (Experiment 6, $C_D=10^{-6}$). Several combinations of the model attributes showed that the best performance is achieved in Experiment 9.

Table 2. Willmot Skill (WS) score for all stations between in situ measurements and simulated SLH from all experiments.

STATION/EXPERIMENT	EXP1	EXP2	EXP3	EXP4	EXP5	EXP6	EXP7	EXP8	EXP9	EXP10	EXP11	EXP12
THESSALONIKI	0.48	0.59	0.53	0.57	0.62	0.53	0.59	0.56	0.68	0.55	0.51	0.65
GENOVA	0.72	0.76	0.76	0.77	0.71	0.73	0.77	0.77	0.79	0.76	0.72	0.61
ANCONA	0.61	0.68	0.68	0.69	0.67	0.63	0.73	0.70	0.72	0.67	0.64	0.69
NAPOLI	0.56	0.62	0.59	0.61	0.59	0.56	0.68	0.66	0.69	0.61	0.56	0.58
MARSEILLE	0.50	0.51	0.55	0.52	0.42	0.51	0.39	0.43	0.46	0.52	0.81	0.46
VENICE	0.61	0.71	0.71	0.72	0.80	0.66	0.75	0.71	0.82	0.69	0.68	0.68
CATANIA	0.40	0.47	0.36	0.43	0.40	0.38	0.45	0.44	0.51	0.43	0.36	0.46
HADERA	0.50	0.54	0.54	0.55	0.62	0.50	0.62	0.65	0.66	0.53	0.51	0.45
CAGLIARI	0.45	0.54	0.47	0.51	0.54	0.48	0.50	0.49	0.60	0.50	0.46	0.43
OTRANTO	0.44	0.53	0.46	0.51	0.52	0.45	0.54	0.51	0.62	0.50	0.43	0.39
ALEXANDROUPOLIS	0.34	0.64	0.63	0.64	0.73	0.59	0.68	0.64	0.77	0.61	0.60	0.76
ALL STATIONS	0.51	0.60	0.57	0.59	0.60	0.55	0.61	0.60	0.67	0.58	0.57	0.56

The Root Mean Square Errors (RMSEs) and the Pearson correlation coefficients were also computed for all experiments and stations. The lowest RMSE for Experiment 9 is computed for the Genova Station as presented in Figure 4. The Willmott skill score for Genova is significantly high (0.79) and the Pearson correlation coefficient (r) of the two timeseries is 0.74.

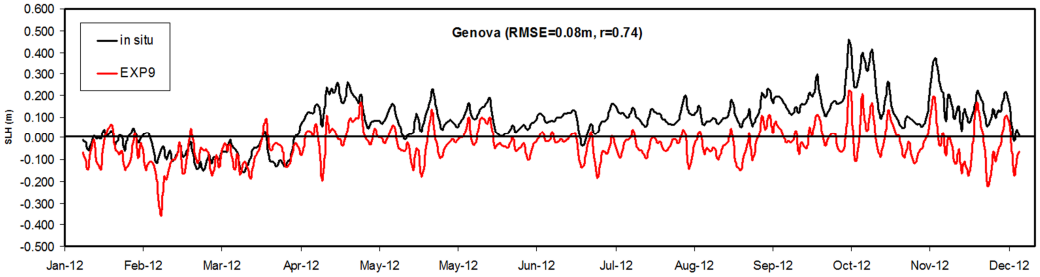

Figure 4. Mean daily evolution of Sea Level Height (SLH) from in situ measurements (black) and HRSS model (red) from Experiment 9 (Table) for 2012 in Genova.

3.1.3 Evaluation of Circulation Simulations

Figure 5 shows the comparison of satellite Sea Surface Temperature (SST) values (L3 multi-sensor SST, with a resolution of 0.02 degrees[k]) and model results for the period of 01/03/2013-31/08/2013, as time-series of spatially averaged values over the entire domain (Fig. 5a) and at characteristic locations in the gulf (Fig.5b-e), as well as in the form of scatter-plot for all locations (5f). The results show that there is good reproduction of the SST temporal evolution, both overall, as well as at distinct areas of the gulf.

For the evaluation the model performance in terms of reproducing SST values, various statistical indicators were calculated and are listed in Table 3. Mean Absolute Error (MAE) values and corresponding Standard Deviations (StDev) are given (in Celsius degrees and normalized), as well as Root Mean Square Error (RMSE) values, Pearson product-moment correlation coefficients (R^2) and WS scores (Eq. [18]). MAE, and, correspondingly, RMSE values are generally low, with very high correlation between measurement and simulation and very good performance of the model, based on the WS values (~1).

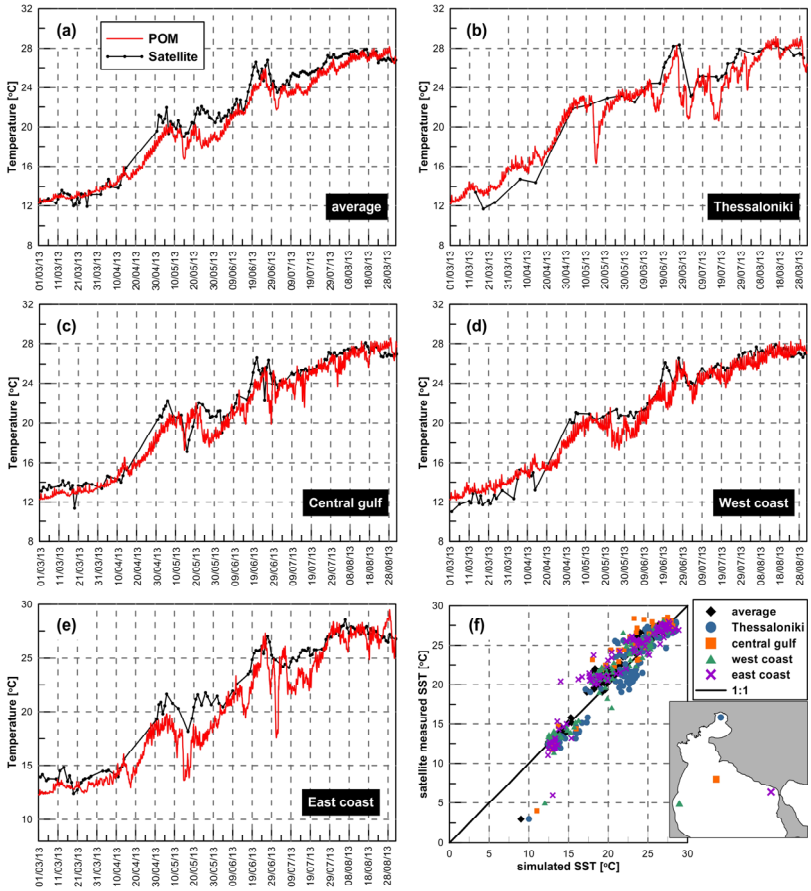

Figure 5. Simulated and satellite SST comparison for: average SST (a) and SST values in the coastal area of Thessaloniki (b), in the central gulf (c) and along the western (d) and eastern (e) coasts and correlation of measured and simulated values of all locations; the locations of the selected stations are noted on the nested map (f) and the availability of satellite recordings is noted with dots (black curve).

[k] http://www.myocean.eu.org/products-services.html

Table 3. Statistical indicators of model performance: Model SST values of Mean Absolute Error (MAE) and Root Mean Square Error (RMSE), correlation coefficient (R^2) and average Willmott Skill (WS) score for the overall gulf and the four, selected, distinct locations.

MODEL PERFORMANCE INDICATORS	AVERAGE	THESSALONIKI	CENTAL GULF	EAST COAST	WEST COAST
MAE±StDev [°C]	0.85±0.96	0.61±1.49	0.71±1.11	0.53±1.23	1.15±1.29
MAE ±StDev [%]	3.60±4.56%	1.67±7.15%	3.21±5.35%	1.47±6.79%	5.42±5.87%
RMSE [°C]	1.28	1.59	1.31	1.33	1.73
R^2	0.97	0.90	0.95	0.95	0.94
Willmott Skill (WS)	0.98	0.97	0.98	0.98	0.97

Due to the lack of measurements in the area regarding salinity values, we compare Sea Surface Salinity (SSS) with satellite measured Chlorophyll-a (Chl-a) concentrations (MODIS-Aqua datasets[I]). It is noted that the use of other modeling results would be inappropriate for comparison, since models in the area, at best, take into account historical monthly values of river outflows from the period 1997-98, in which two of the Aliakmon dams were not yet constructed. The comparison of SSS model results and satellite Chl-a concentrations are given in figure 6, as spatial distribution of the values for 2, indicative, simulation days (Fig. 6a-d) and as scatter plot of the 2 parameters from the whole time-series at the location of the river outflows (Fig. 6e). It is noted that the coloring used in the contour plots (Fig. 6a-d) was selected so as to facilitate the reader (low-salinity waters should coincide with high concentrations of Chl-a and vice-versa). It can be noted that the form of the hyposaline and Chl-a-rich water 'plumes' generally compare well in terms of morphology and spreading, while low-salinity waters correspond to locations of peak Chl-a concentrations. Regarding the comparison of the whole time-series at the river outflows, it is noted that the correlation is obviously far from perfect; however, a general inverse relationship between the two parameters can be identified. The large scattering of the two parameters is attributed mainly to the fact that the relationship of the two parameters is not necessarily linear; factors other that hyposaline, and usually nutrient-rich, waters can increase primary productivity, like temperatures, on-riverine sources of nutrients, nitrate to phosphate ratios etc.

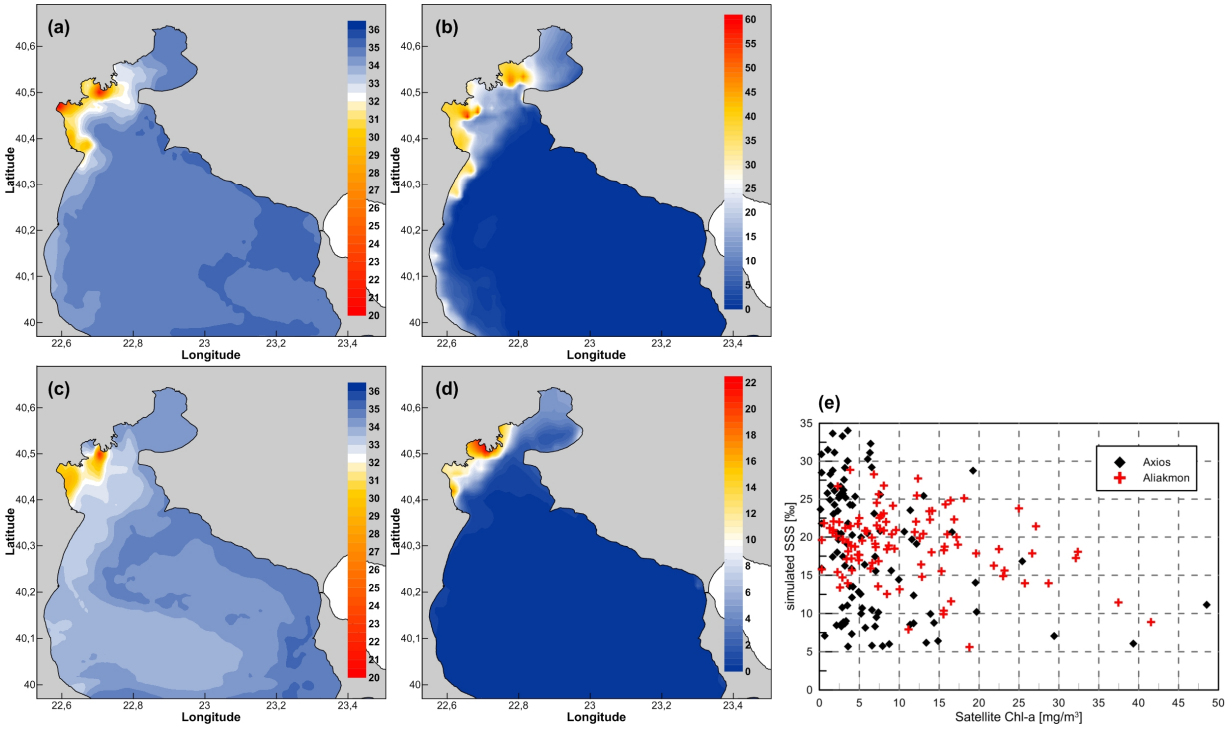

Figure 6. Simulated SSS (a and c) and satellite Chl-a concentrations (b and d) [mg/m^3] for 05/03 (top) and 09/06 and comparison of SSS values versus satellite Chl-a concentrations (mg/m^3) at the outflows of the two main rivers, Axios and Aliakmon (e).

3.2. 3-day forecasts

Based on the calibrated models, as derived from the hind-casting simulations presented above, the 3-day forecasting simulations provide daily sea-state products. A variety of different forecast parameters are disseminated through the dissemination system of WaveForUs (Fig. 1), including horizontal spatial distributions of significant wave height and direction, SLHs, temperature, salinity and current velocity fields at 0m, 20m, 40m and at the seabed, as well as time-series of the products at selected point of interest in the gulf.

[I] http://modis.gsfc.nasa.gov/data/

For example, the prediction of SLH in a 3-hourly time-step during a 3-day forecast in Thessaloniki (north Gulf) and Fourka (south Gulf) stations is presented in Figure 7.

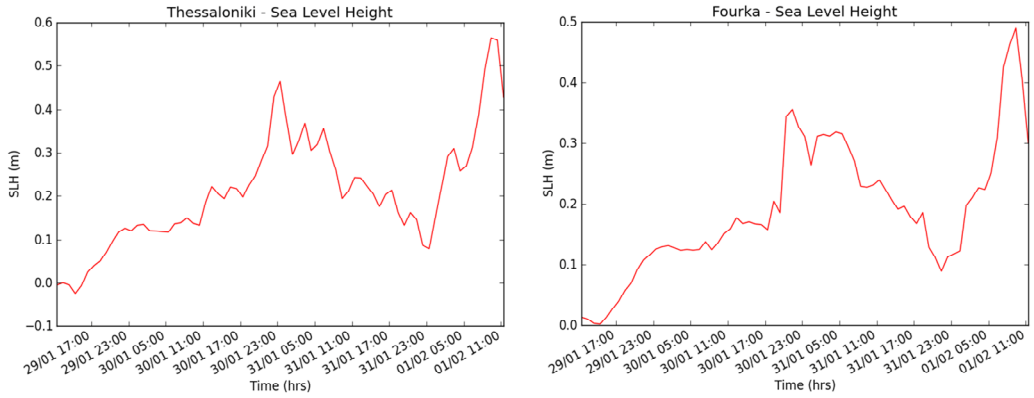

Figure 7. 3-hourly forecasts of Sea Level Height (SLH) at Thessaloniki (left panel) and Fourka (right panel) stations, covering the period from 29/01/2015 to 01/02/2015.

Although the SLH are low in the beginning of the forecast, significantly high values are calculated in end of the 3-day period, while the temporal variation of SLH is similar at both stations. The northern Thessaloniki station reveals 5 cm greater peak due to the accumulation of waters in the inner Gulf under the forcing of strong southerly winds (14 m/sec, Fig. 8). Respective forecast products of wave characteristics and circulation parameters in several depths are daily available from the WaveForUS system. The higher horizontal and vertical resolution of the system in comparison with similar existing operational systems (see Section 1) provides more detailed and efficient sea-state products in Thermaikos Gulf.

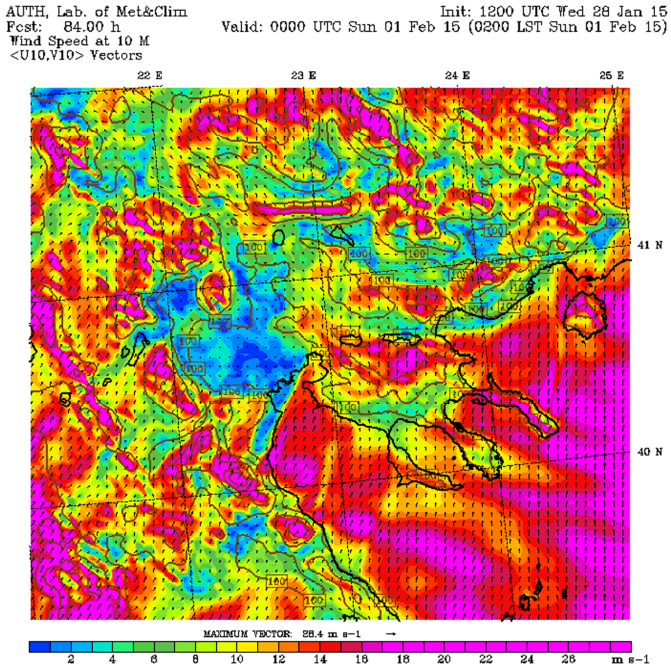

Figure 8. 10m wind speed (m/s) and direction from the WRF-ARW model over the northern Greece on 01/02/2015 [source: http://meteo.geo.auth.gr].

4. CONCLUSIONS

The validation of the models with available in situ observations and satellite data showed that the operational WaveForUs system is an adequate and useful tool on the prediction of the short-term sea-state in Thermaikos Gulf. The integrated management of the coastal zone of Thermaikos Gulf with extensive urban, agriculture, tourist, and industrial infrastructures requires efficient operational forecasting products, focused in the different areas and uses of the area. The high resolution of the WaveForUs system accomplishes this requirement. The simulation of severe meteorological events that may induce inundation phenomena over low-land areas provides a daily alerting system along the entire

coastal zone. Specific state of the art parameterizations such as the computation of the astronomical tide or the river outflow estimation improved the performance of the simulations. The wide range of sea-state products, provided to the public with several different ways, covers the different needs of potential users in the complicated Thermaikos environment under the high spatial and temporal resolution.

ACKNOWLEDGMENTS

The WaveForUs project is funded by the national action 'COOPERATION 2011:' Partnerships of Production and Research Institutions in Focused Research and Technology Sectors in the framework of the operational programme 'Competitiveness and Entrepreneurship' (NSRF2007-2013) and is implemented by: (a) the Laboratory of Maritime Engineering and Maritime Works of the A.U.Th., (b) the company OMIKRON Ltd., Planning, Study and Management of Environmental and Technical Works, (c) DION TV, (d) the Laboratory of Meteorology and Climatology of A.U.Th. and (e) the Region of Central Macedonia. The WaveForUs system uses MyOcean (http://www.myocean.eu/) products.

REFERENCES

Abdalla S. and Bidlot J.R. (2002). Wind gustiness and air density effects and other key changes to wave model in CY25R1. *Tech. Rep. Memomrandum R60.9/SA/0273*, Research Department, ECMWF, Reading, U. K.

Battjes J.A. and Janssen J.P.F.M. (1978). Energy loss and set-up due to breaking of random waves. *Proc. 16th Int. Conf. Coastal Engineerging*, ASCE, 569–587

Bretherthon F.P. and Garrett C.J.R. (1968). Wave trains in inhomogeneous moving media. *Proc. Roy. Soc. London*, A 302, 529–554.

Blumberg A.F. and Mellor G.L. (1987). A description of a three-dimensional coastal ocean circulation model. *Three-Dimensional Coastal Ocean Models*, Ed. N.S. Heaps, American Geophysical Union, Washington, DC, pp. 1-16.

De Vries H., Breton M., Mulder T., Krestenitis Y., Ozer J., Proctor R., Ruddick K., Salomon J.C. and Voorrips A. (1995). A comparison of 2D storm surge models applied to three shallow European seas. *Environmental Software*, 10, 23–42.

Korres G., Nittis K., Hoteit I. and Triantafyllou G. (2008). A high resolution data assimilation system for the Aegean Sea hydrodynamics. *Journal of Marine Systems*, 77, 325–340.

Krestenitis Y.N., Androulidakis Y., Kontos Y. and Georgakopoulos G. (2011). Coastal inundation in the north-eastern Mediterranean coastal zone due to storm surge events. *Journal of Coastal Conservation*, 15, 353–368.

Latinopoulos, P. and Krestenitis, Y. 2001. *Land-water reclamation works*, AUTh, 129 pp.

Lionello P., Malanotte-Rizzoli P., Boscolo R., Alpert P., Artale V., Li L., ..., Xoplaki E. (2006). The Mediterranean climate: an overview of the main characteristics and issues. *Developments in earth and environmental sciences*, 4, 1-26.

Liu Y., MacCready P., Hickey B.M., Dever E.P., Kosro P.M., Banas N.S. (2009). Evaluation of a coastal ocean
circulation model for the Columbia River plume in summer 2004. *Journal of Geophysical Research*, 114, C00B04, doi:10.1029/2008JC004929.

Lowe P.R. (1977). An approximating polynomial for the computation of saturation vapor pressure. *Journal of Applied Meteorology*, 16, 100–103.

Pytharoulis I., Tegoulias I., Kotsopoulos S., Bampzelis D., Karacostas Th. and Katragkou E. (2014). Evaluation of the Operational Numerical Weather Predictions of the WaveForUs project, Proceedings of the 12th International Conference on Meteorology, Climatology and Atmospheric Physics 2014, pp. 96-101.

Rosati A. and Miyakoda K. (1988). A general circulation model for upper ocean simulation. *Journal of Physical Oceanography*, 18, 1601–1626.

Schwiderski E.W. (1980). On charting global ocean tides. *Reviews of Geophysics*, 18(1), 243-268.

Smith S.D. and Banke E.G. (1975). Variation of the sea surface drag coefficient with wind speed. *Quarterly Journal of the Royal Meteorological Society*, 101(429), 665-673.

Tolman H.L. (2002a) Alleviating the garden sprinkler effect in wind wave models. *Ocean Mod.*, 4, 269–289.

Tolman H.L. (2006). Toward a third release of WW III; a multi-grid model version. *Proc. 9th international workshop on wave hindcasting and forecasting*, JCOMM Tech. Rep. 34. Paper L1.

Tolman H.L. (2007). Development of a multi-grid version of WW III. *Tech. Note 256*, NOAA/NWS/NCEP/MMAB, 88 pp. + Appendices.

Tolman H.L. (2008). A mosaic approach to wind wave modeling. *Ocean Mod.*, 25, 35–47.

USACE (2000). Design of spillway Tainter gates. *Engineer Manual 1110-2-2702* - U.S. Army, 113 pp.

Wang W., Bruyère C., Duda M., Dudhia J., Gill D., Lin H.-C., Michalakes J., Rizvi S., Zhang X., Beezley J., Coen J. and Mandel J. (2010). ARW Version 3 Modeling System User's Guide, *NCAR-MMM*, 354 pp.

Weare B.C., Strub P.T., Samuel M.D. (1981). Annual Mean Surface Heat Fluxes in the Tropical Pacific Ocean. *Journal of Physical Oceanography*, 11, 705–717.

Whitham G.B. (1965). A general approach to linear and non-linear dispersive waves using a Lagrangian. *J. Fluid Mech.*, 22, 273–283.